

1 **Title:**

2 Unraveling the effects of spatial variability and relic DNA on the temporal dynamics of  
3 soil microbial communities  
4

5  
6 **Authors:**

7 Paul Carini<sup>1,2</sup>, Manuel Delgado-Baquerizo<sup>1,3</sup>, Eve-Lyn S. Hinckley<sup>4,5</sup>, Tess E Brewer<sup>1,6</sup>,  
8 Garrett Rue<sup>4</sup>, Caihong Vanderburgh<sup>1</sup>, Diane McKnight<sup>4</sup> and Noah Fierer<sup>1,7</sup>  
9

10 **Affiliations:**

11 <sup>1</sup> Cooperative Institute for Research in Environmental Sciences, University of Colorado,  
12 Boulder, CO 80309

13 <sup>2</sup> Current Address: Department of Soil, Water and Environmental Science, University of  
14 Arizona, Tucson, AZ 85721

15 <sup>3</sup> Departamento de Biología y Geología, Física y Química Inorgánica, Escuela Superior  
16 de Ciencias Experimentales. Universidad Rey Juan Carlos, c/ Tulipán s/n, 28933  
17 Móstoles, Spain.

18 <sup>4</sup> Institute of Arctic and Alpine Research, 4001 Discovery Dr, Boulder, CO 80303

19 <sup>5</sup> Environmental Studies Program, 4001 Discovery Dr, Boulder, CO 80303

20 <sup>6</sup> Department of Molecular, Cellular, and Developmental Biology, University of Colorado,  
21 Boulder, Colorado 80309, USA.

22 <sup>7</sup> Department of Ecology and Evolutionary Biology, University of Colorado, Boulder, CO  
23 80309  
24

25 **Corresponding authors:**

26 paulcarini@email.arizona.edu or noah.fierer@colorado.edu  
27

28 **Keywords:** Microbial seasonality, soil microbial ecology, microbial interactions  
29

30 **Abstract:**

31 Few studies have comprehensively investigated the temporal variability in soil microbial  
32 communities despite widespread recognition that the belowground environment is  
33 dynamic. In part, this stems from the challenges associated with the high degree of  
34 spatial heterogeneity in soil microbial communities<sup>1</sup> and because the presence of relic  
35 DNA<sup>2</sup> may mask temporal dynamics. Here we disentangle the relationships among  
36 spatial, temporal, and relic DNA effects on microbial communities in soils collected from  
37 contrasting hillslopes in Colorado, USA. These sites were chosen because they have  
38 distinct soil microbial communities and experience strong seasonal changes in  
39 precipitation and temperature regimes. We intensively sampled plots on each hillslope  
40 over one year to discriminate between temporal variability, the intra-plot spatial  
41 heterogeneity, and relic DNA effects on the soil prokaryotic and fungal communities. We  
42 show that the intra-plot spatial variability in microbial community composition was strong  
43 and independent of relic DNA effects and these spatial patterns persisted throughout  
44 the study. When controlling for intra-plot spatial variability, we identified significant  
45 temporal variability in both plots, particularly after relic DNA was removed, suggesting  
46 that relic DNA hinders the detection of important temporal dynamics in soil microbial

47 communities. We also identified microbial taxa that exhibited shared temporal  
48 responses and we show that these responses were often predictable from temporal  
49 changes in soil conditions. These findings highlight approaches that can be used to  
50 better characterize temporal shifts in soil microbial communities, information that is  
51 critical for predicting the environmental preferences of individual soil microbial taxa and  
52 identifying linkages between soil microbial community composition and belowground  
53 dynamics.

54

## 55 **Introduction:**

56 Information on the temporal dynamics of microbial communities over different  
57 time scales can be used to better understand the factors influencing the structure of  
58 microbial communities and their contributions to ecosystem processes. We know that  
59 the microbial communities found in the human gut<sup>3</sup>, leaf litter<sup>4</sup>, marine<sup>5</sup>, and freshwater<sup>6</sup>  
60 habitats can exhibit a high degree of temporal variation. Although the magnitude and  
61 timing of this temporal variation in community composition can vary depending on the  
62 environment and taxon in question, such temporal variability is often predictable from  
63 environmental factors<sup>7</sup>. For example, ocean microbial communities display predictable  
64 periodic oscillations over time (seasonality) that has been linked to regular changes in  
65 biotic and abiotic factors, including phytoplankton dynamics and physicochemical  
66 factors (reviewed in refs<sup>5,8</sup>). These changes in environmental conditions influence the  
67 nature of biotic interactions within these ecosystems and can have important  
68 ramifications for understanding the functional attributes of microbial communities and  
69 the ecosystem services they provide<sup>9-11</sup>.

70 Understanding how temporal changes in environmental conditions influence soil  
71 microbial communities is necessary to accurately model how microbial communities  
72 contribute to soil processes and for using microbes as bio-indicators of changes in  
73 belowground conditions such as carbon and nutrient availability – parameters that are  
74 often difficult to measure directly. However, results from previous studies of temporal  
75 variability in soil microbial communities are idiosyncratic. While some studies show soil  
76 microbial communities exhibit measurable temporal variation in response to  
77 experimental warming<sup>12,13</sup> and seasonal patterns in temperature and moisture<sup>14-18</sup>, other  
78 studies show no or minimal variation over time, despite marked changes in  
79 environmental conditions<sup>7,19,20</sup>. One possible explanation for the discrepancies across  
80 studies is that the spatial heterogeneity in soil microbial communities – even across  
81 short distances – can be sufficiently large to obscure temporal patterns. This hypothesis  
82 is supported by numerous studies demonstrating that the spatial variability in soil  
83 microbial communities (even across locations only a few meters apart) can be large (for  
84 example, ref. <sup>1</sup>). Another explanation is that relic DNA – legacy DNA from dead  
85 microbes that can persist in soil – may dampen the observed temporal variability by  
86 effectively hiding the true temporal dynamics of soil microbial communities. Relic DNA is  
87 abundant in soil<sup>2,21</sup>, and models suggest that during microbial community turnover relic  
88 DNA can mask changes in community structure<sup>21</sup>.

89 We conducted a yearlong study aimed at disentangling the spatial and relic DNA  
90 effects on temporal dynamics in belowground microbial communities. Our study sites  
91 were soils on opposing hillslope aspects of a montane ecosystem within the Colorado  
92 Front Range of the Rocky Mountains. We intensively sampled two 9 m x 9 m plots,

93 divided into 3 m × 3 m sub-plots, located in the Gordon Gulch subcatchment within the  
94 Boulder Creek Critical Zone Observatory (BcCZO) every 40-55 days from November  
95 2015 to November 2016 (Fig. 1; nine time points total). We chose these locations  
96 because the soil microbial communities on the two hillslopes are compositionally  
97 distinct<sup>2</sup>, relic DNA is abundant (40-60% of the total soil DNA pool, ref. <sup>2</sup>), and the two  
98 sites undergo strong seasonal changes in moisture and temperature<sup>22</sup>. Moreover, the  
99 temperature and moisture regimes are distinct across the two slopes<sup>22</sup>, providing us  
100 with naturally contrasting systems in which to investigate temporal dynamics in  
101 belowground microbial communities. We characterized the microbial communities at  
102 each site using 16S rRNA gene and internal transcribed spacer 1 (ITS) marker  
103 sequencing to profile the prokaryotic and fungal communities, respectively. Here, we  
104 unravel the relationships between spatial and temporal variability in microbial  
105 community composition, and show the effects of relic DNA on these apparent sources of  
106 variability. Further, we use this information on temporal dynamics to identify groups of  
107 microbes that share temporal patterns and similar responses to changes in  
108 environmental conditions, information that provides novel insight into the ecologies of  
109 understudied soil microbial taxa.

110

## 111 **Results & Discussion:**

112 **Spatial variation in soil microbial communities is unaffected by relic DNA and**  
113 **stronger than temporal variation.** Consistent with previous studies conducted at these  
114 sites<sup>2</sup>, and other studies describing the spatial variability of soil microbial communities<sup>1</sup>,  
115 the prokaryotic and fungal communities on the south-facing hillslope (SFS) were distinct  
116 from those on the north-facing hillslope (NFS), regardless of the time point sampled or  
117 whether relic DNA was removed (Supplementary Fig. 1). Most notably, the SFS had  
118 higher relative abundances of the archaeal phylum Crenarchaeota (all of which were  
119 classified as probable ammonia-oxidizing '*Candidatus Nitrososphaera*'), and the  
120 bacterial phyla Nitrospirae and Verrucomicrobia (Supplementary Fig. 2). Beyond these  
121 expected slope-scale differences, we observed significant intra-plot spatial  
122 heterogeneity in microbial community composition that persisted throughout the course  
123 of the experiment, and this intra-plot heterogeneity was evident irrespective of whether  
124 relic DNA was removed. Before removing relic DNA, there was significant spatial  
125 variability across the sub-plots in both prokaryotic and fungal communities on the NFS  
126 (Fig. 2 a,e; PERMANOVA  $R^2=0.192$  and  $R^2=0.328$ ;  $P\leq 0.001$ , respectively). Significant  
127 spatial differences were still apparent on the NFS for both prokaryotes and fungi after  
128 relic DNA was removed (Fig. 2 c,g; PERMANOVA  $R^2=0.180$  and  $R^2=0.287$ ;  $P\leq 0.001$ ,  
129 respectively). We also found significant spatial variability on the SFS in samples that  
130 were not treated to remove relic DNA, but this spatial effect was much more  
131 pronounced than the NFS, with a clear partitioning between sub-plots 5, 6, 8 and 9 (see  
132 'Plot Design' in Fig. 1a for numbering) from the remainder of the sub-plots (Fig. 2 b,f;  
133 PERMANOVA  $R^2=0.511$ ,  $P\leq 0.001$  for prokaryotes and  $R^2=0.331$ ,  $P\leq 0.001$  for fungi).  
134 Similar to the NFS, these strong spatial patterns remained after relic DNA was removed  
135 (Fig. 2 d,h; PERMANOVA  $R^2=0.498$  for prokaryotes and  $R^2=0.290$  for fungi;  $P\leq 0.001$ ).  
136 These data show that the spatial variability in soil microbial community composition on  
137 the meter scale persists over time and that the presence of relic DNA does not affect  
138 our ability to detect this persistent spatial variation.

139

140 **Removing relic DNA enhanced our ability to detect temporal changes in soil**  
141 **microbial communities.** We investigated the temporal variability in belowground  
142 microbial communities, and the effect of relic DNA on this temporal variability, on a sub-  
143 plot basis to control for the aforementioned high degree of intra-plot spatial variability  
144 and discriminate between temporal and spatial sources of variation in microbial  
145 community structure. When limiting PERMANOVA permutations to within sub-plots over  
146 time, we found significant temporal variability for both prokaryotes and fungi in both  
147 untreated control soils (PERMANOVA  $R^2=0.187$   $P\leq 0.001$  for prokaryotes and  $R^2=0.147$   
148  $P\leq 0.001$  for fungi on the NFS; and  $R^2=0.123$   $P\leq 0.001$  for prokaryotes and  $R^2=0.123$   
149  $P\leq 0.001$  for fungi on the SFS) and soils that were treated to remove relic DNA  
150 (PERMANOVA  $R^2=0.177$   $P\leq 0.001$  for prokaryotes and  $R^2=0.141$   $P\leq 0.001$  for fungi on  
151 the NFS; and  $R^2=0.108$   $P\leq 0.001$  for prokaryotes and  $R^2=0.157$   $P\leq 0.001$  for fungi on  
152 the SFS). However, on average, the fungal communities on both slopes, and prokaryotic  
153 communities on the NFS were significantly more dissimilar over time after relic DNA  
154 was removed, compared to untreated control soils that contained relic DNA (Fig. 3;  
155 Kruskal-Wallis test  $P\leq 0.05$ ). These results indicate that, while temporal signals in soil  
156 microbial communities can be identified in the presence of relic DNA, the removal of  
157 'legacy' DNA from dead microbes that can persist in soil significantly enhances the  
158 ability to detect important temporal variation in the composition of soil microbial  
159 communities.

160

161 **Temporal variability in distinct assemblages of prokaryotes and fungi are**  
162 **predictable from soil variables.** Characterizing shifts in the relative abundances of  
163 individual microbial taxa in temporally dynamic soil systems can give important insight  
164 into the ecologies of individual taxa and, more generally, the environmental factors that  
165 influence belowground communities. Thus, we next sought to identify specific groups of  
166 taxa that exhibited correlated changes in relative abundances over time in soils after  
167 relic DNA was removed. To do this, we used local similarity analysis (LSA)<sup>23</sup> to identify  
168 strong (local similarity score  $\geq 0.7$ ) and significant (q-value  $\leq 0.001$ ) positive pairwise  
169 microbe-microbe temporal correlations. We constructed and analyzed networks from  
170 these correlations and extracted distinct groups (modules) of microbes from NFS and  
171 SFS networks using modularity analysis<sup>24</sup> (Fig. 4). On the NFS, the mean normalized  
172 relative abundances of 292 microbial taxa (184 bacteria and 108 fungi) were  
173 significantly correlated with at least one other taxon over time (Fig. 4a). These  
174 correlated taxa clustered into seven modules – the mean normalized relative  
175 abundances of four of these modules changed significantly with time and displayed  
176 distinct temporal trajectories (Fig. 4b). On the SFS, 291 taxa (1 archaeon, 191 bacteria  
177 and 99 fungi) were included in the network, and clustered into six modules (Fig. 4c).  
178 The relative abundances of three of these six SFS modules changed significantly with  
179 time (Fig. 4d).

180 A large proportion of the temporal variation in the mean normalized relative  
181 abundances of the modules that were found to change significantly over time could be  
182 explained by temporal variation in measured soil or environmental characteristics. At  
183 each time point, we measured a suite of soil and environmental parameters, including:  
184 snow depth, soil temperature and moisture, extractable inorganic nitrogen ( $\text{NO}_3^- +$

185  $\text{NH}_4^+$ ), salinity (electrical conductivity), extractable phosphorus (P), pH, and the  
186 chromophoric properties of water-soluble organic matter (WSOM; a metric of organic  
187 matter lability<sup>25</sup>). These measured soil characteristics explained 12 to 76% of the  
188 variance in the mean normalized relative abundance of a given module (Supplementary  
189 Fig. 3). We identified two sets of modules that differed in the specific factors that  
190 predicted temporal variation. The first set of modules, containing modules 0, 3, 7 and  
191 12, were best predicted by climactic variables, most notably soil temperature and  
192 moisture and snow depth (Supplementary Fig. 3). These results are in line with previous  
193 studies demonstrating how changes in soil temperature<sup>12,16-18</sup>, moisture<sup>26</sup> and snow  
194 pack<sup>14</sup> can influence belowground microbial communities. In contrast, modules 1, 2 and  
195 11 were best explained by changes in inorganic nutrient concentrations (nitrogen and  
196 phosphorus; Supplementary Fig. 3). While nitrogen and phosphorus inputs can have  
197 predictable<sup>27</sup> and lasting<sup>4</sup> effects on microbial community structure, we have a more  
198 limited understanding of how short-term seasonal variation in the availability of these  
199 nutrients can influence microbial community dynamics, despite evidence that  
200 belowground microbial communities are important mediators of soil nutrient  
201 dynamics<sup>28,29</sup>. Our results show that a subset of soil microbes organize into modules  
202 that are responsive to these subtle changes in nitrogen and phosphorus availability.  
203 Variability in WSOM constituents did not contribute significantly to temporal variability in  
204 environmental conditions (Supplementary Fig. 4) and thus, we excluded these  
205 measures from the models describing the temporal variability of the modules. Given that  
206 previous work at these sites showed a high degree of spatial variation in WSOM  
207 distributions<sup>25,30</sup>, we suspect that the pronounced spatial variability in WSOM  
208 distributions may have obscured our ability to detect significant effects of WSOM  
209 characteristics on the temporal dynamics of the soil microbial communities.

210 The construction of modules based on shared temporal patterns allowed us to  
211 identify biotic or abiotic factors that are correlated with shifts in the relative abundances  
212 of individual taxa. For example, similar to studies showing that ammonia-oxidizing  
213 archaea are particularly sensitive to changes in temperature<sup>31</sup> and pH<sup>32,33</sup>, we found that  
214 both temperature and pH were good predictors of the temporal distribution of module  
215 12, which contained ammonia-oxidizing thaumarchaea (Fig. 4d and Supplementary Fig.  
216 3). Because nitrification is often a coupled process – the oxidation of ammonium to  
217 nitrite by ammonia oxidizers, and the subsequent oxidation of nitrite to nitrate by nitrite  
218 oxidizers – we were surprised that probable nitrite-oxidizing Nitrospirae were not  
219 temporally correlated with these thaumarchaea, but were instead a part of a distinct  
220 module (module 8; Fig. 4d) that did not change significantly over time. As observed in  
221 some marine systems<sup>34,35</sup>, we suspect that nitrification in SFS soils may be periodically  
222 uncoupled, though more work is necessary to test this hypothesis.

223 Our study also provides insight into the short-term temporal variation of  
224 ectomycorrhizal communities, the environmental factors that influence these patterns  
225 and other fungal and prokaryotic taxa that co-vary with ectomycorrhizal fungi.  
226 Ectomycorrhizal fungi were found on both slopes and partitioned into several modules  
227 that were significantly variable over time (modules 0, 1, 2, 3, 7, 11, and 12 in Fig. 4;  
228 Supplementary Table 1). Interestingly, some of these modules were best predicted by  
229 climactic variables (Supplementary Fig. 3; for example, those ectomycorrhizal fungi  
230 found in modules 3 and 7). Modules 3 and 7 had peak abundances in the summer

231 months (Fig. 4), suggesting that the abundances of these ectomycorrhizal taxa were  
232 elevated during months when plant productivity peaks. However, other ectomycorrhizal  
233 fungi were found in modules best predicted by nutrient availability. These findings  
234 indicate a degree of temporal niche partitioning in ectomycorrhizal fungal communities  
235 on both slopes in response to distinct environmental conditions (Supplementary Fig. 3)

## 236 237 **Conclusions:**

238 This study provides new evidence that the temporal dynamics of groups of  
239 prokaryotes and fungi are predictable in terrestrial ecosystems, and that a more detailed  
240 characterization of the temporal variability in soil microbial communities is critical to  
241 understanding the dynamic nature of the soil microbiome. The extensive spatial and  
242 temporal sampling design of our study allowed us to disentangle the relationships  
243 among spatial heterogeneity in microbial communities, temporal dynamics of these  
244 communities, and the effect of relic DNA on these temporal patterns. Unsurprisingly,  
245 spatial variation in community structure at both the hillslope scale, and the meter scale  
246 (intra-plot) was the dominant source of variability in this study and relic DNA had no  
247 significant effect on these patterns (Supplementary Fig. 1 and Fig. 2).

248 When controlling for this spatial variability, we were able to detect significant  
249 temporal shifts in microbial community composition, regardless of whether relic DNA  
250 was removed or not. We emphasize that the magnitude of the temporal variation in soil  
251 microbial communities was consistently lower than the spatial variation, even between  
252 sub-plots located only a few meters apart. This spatial variability in surface soil microbial  
253 communities was relatively stable over time, suggesting that efforts to describe spatial  
254 variation in overall community composition do not necessarily need to include samples  
255 collected across multiple time points.

256 We also provide new evidence that the removal of relic DNA enhances our ability to  
257 detect temporal patterns in the belowground communities. These findings support our  
258 previous hypothesis<sup>2</sup>, and predictions based on modeling<sup>21</sup>, that relic DNA can conceal  
259 temporal patterns in soil microbial communities. The presence of relic DNA, even in high  
260 amounts, does not automatically lead to relic DNA biases in other ecosystems<sup>21</sup>.  
261 However, our data do suggest that relic DNA has important effects on studies of  
262 temporal variation in soil microbial communities (and possibly in other ecosystems), and  
263 that the consequences of failing to remove relic DNA would not be apparent from single  
264 time point samples.

265 The belowground environment is one of the most complex and dynamic microbial  
266 habitats on Earth. By controlling for spatial and relic DNA effects on temporal variability  
267 in these soil microbial communities, we identified groups of microbes that have similar  
268 temporal dynamics and the factors that predicted their temporal distributions. A deeper  
269 understanding of relationships between soil microbiota can help resolve both the roles  
270 of individual taxa and potential 'ecological clusters' with emergent function. For  
271 example, taxa that covary may exhibit similar niche preferences and compete for growth  
272 substrates. In contrast, taxa belonging to a given module may broadly cue in on similar  
273 environmental signals but occupy distinct substrate niches<sup>36</sup>. Alternatively, microbes that  
274 are correlated over time may interact through cross-feeding of metabolic substrates or  
275 co-utilization of leaky functions<sup>37</sup> - either directly or in a time-lagged manner.  
276 Understanding the basis for shared temporal dynamics is important as microbial

277 interactions are crucial in shaping microbial communities<sup>38</sup> but difficult to measure  
278 directly<sup>39</sup>. Future investigations that combine cell culture, synthetic microbial  
279 communities and genomics may help resolve the specific drivers of these co-occurrence  
280 patterns<sup>36,40</sup>.

281

## 282 **Methods:**

283 *Site description, plot design and sampling procedure:* The two plots were set up  
284 on opposing slopes alongside an instrumented transect near the rain-snow transition at  
285 ~2,530 meters elevation (approximately 40.01°N, 105.47°W), chosen on the expectation  
286 that there would be a high level of temporal variability in soil microbial communities as a  
287 result of intra-annual changes in soil moisture and temperature<sup>22</sup>. The north-facing slope  
288 (NFS) and south-facing slope (SFS) have distinct soil and vegetation characteristics and  
289 experience different water delivery patterns, particularly during snowmelt<sup>22</sup> (Fig. 1). The  
290 NFS and SFS soils are Ustic dystrocryept (Catamount series) and Lithic haplstoll,  
291 respectively<sup>41</sup>. Soil moisture and temperature were variable over the course of the study  
292 and followed expected seasonal trends (Fig. 1). In general, the NFS had a higher soil  
293 moisture and a lower temperature than the SFS (Fig. 1). The NFS is vegetated with  
294 moderately dense *Pinus contorta* (Lodgepole pines) and develops a snowpack during  
295 the winter that melts in spring. In contrast, the SFS is much more sparsely vegetated  
296 with *Pinus ponderosa* (Ponderosa pines), intervening grasses and *Arctostaphylos uva-*  
297 *ursi* (kinnikinnick) shrubs and experiences pulses of snowmelt throughout the winter and  
298 spring. We sampled ~10-15 random soil cores (0-5 cm, mineral soils only; 1" core  
299 diameter) within each sub-plot at each of the nine time points. The soil cores from each  
300 sub-plot were pooled, sieved to 2 mm and homogenized at each time point and  
301 partitioned for microbial community and nutrient analyses. Sample dates are reported in  
302 Supplementary Table 2. Sampling for the July 2016 sample was delayed by ~7 days  
303 because a nearby wildfire prevented site access.

304

305 *Continuous environmental measurements:* Several automated measurements  
306 were collected every 10 minutes at a meteorological station located near the sample  
307 sites (see 'Data availability' for data source information). Each slope was instrumented  
308 with a soil temperature sensor (Campbell Scientific T-107 temperature probe), and a  
309 soil water content reflectometer (Campbell Scientific CS616) located 5 cm below  
310 ground. The daily averages from these sensors on each slope are illustrated in Fig.  
311 1b,c. When modelling the relative mean importance of temperature and volumetric  
312 water content to module temporal distributions, we used the average of daily mean  
313 values from these sensors between sample dates, except for the first time point, which  
314 is the mean from the preceding 34 days. Snow depth was measured using digital  
315 ultrasonic snow depth sensors (Judd Communications Inc.) fitted with CR1000  
316 dataloggers (Campbell Scientific). Snow depth is reported as mean daily snow depth  
317 between sampling points from three sensors on each slope (NFS at snow pole 3,  
318 sensors 1-3 and SFS snow pole 10, sensors 9, 11 and 15).

319

320 *Discrete environmental measurements:* Inorganic N pools were measured for  
321 each sub-plot at each time point except for the January 2016 sample on the NFS, sub-  
322 plots 1 and 2 and SFS sub-plot 3, where insufficient soil was collected. Sieved soils for

323 inorganic N analyses were stored at 4°C for <72 h. Inorganic N pools were extracted  
324 from 10 g field-moist soil in 100 mL 2M potassium chloride with periodic shaking for 18  
325 h and filtered through cellulose Whatman 1 filters. Ammonium (NH<sub>4</sub><sup>+</sup>) was measured  
326 from these extracts on a BioTek Synergy 2 with a detection limit of 0.009 mg N L<sup>-1</sup> and  
327 nitrate (NO<sub>3</sub><sup>-</sup>) was measured on an OI Analytical FS-IV with a detection limit of 0.5603  
328 µg N L<sup>-1</sup>. Dissolved inorganic nitrogen (DIN) was calculated as the sum of NH<sub>4</sub><sup>+</sup> and  
329 NO<sub>3</sub><sup>-</sup>.

330 Water-soluble organic matter (WSOM) was analyzed for each sub-plot at each time  
331 point except for the following plots, where insufficient sample was collected: NFS  
332 February 2016 (all sub-plots), July 2016 sub-plot 1, August 2016 sub-plots 1-7,  
333 November 2016 sub-plots 1, 2 and 5; and SFS February 2016 sub-plots 1, 8 and 9 and  
334 April 2016 sub-plot 5. Sieved soils were stored at -20°C until WSOM extraction. WSOM  
335 was extracted by leaching 10 g of soil with 50 ml 0.5 M K<sub>2</sub>SO<sub>4</sub> following the methods  
336 described in<sup>25</sup>. The spectroscopically-active portion of the WSOM was characterized  
337 with UV-Vis and fluorescence spectroscopy. Samples were diluted to minimize the inner  
338 filter effect<sup>42</sup> and the UV-Vis absorbance was measured from 200-800 nm in 1 nm  
339 increments using an Agilent 8453 Spectrophotometer with a 1 cm path  
340 length. Dissolved organic carbon (DOC) and total nitrogen were measured on a  
341 Shimadzu TOC-V. SUVA<sub>254</sub>, a proxy for the aromaticity of the WSOM, was calculated  
342 as the absorbance at 254 nm normalized by the DOC concentration<sup>43</sup>. Fluorescence  
343 scans were collected on a Horiba Jobin Yvon Fluoromax-4 with a 1 cm quartz cuvette  
344 and normalized to Raman units<sup>44</sup>. The fluorescence index (FI)<sup>45</sup> and humification index  
345 (HIX)<sup>46</sup> were calculated from the fluorescence scans using Parallel Factor Analysis  
346 (PARAFAC) to further resolve discrete components representing different classes of  
347 fluorophores<sup>25</sup>.

348 Other standard soil characteristics were measured at each time point by pooling  
349 equal masses of soil from each sub-plot plot on each slope. These measurements  
350 included: pH, electrical conductivity (mmhos cm<sup>-1</sup>) and P (ppm). Standard soil chemical  
351 analyses were performed at the Colorado State University Soil Water and Plant Testing  
352 Laboratory using their standard protocols.

353 *Relic DNA removal and DNA extraction:* Relic DNA was removed as described  
354 previously<sup>2</sup>. Briefly, 0.03 g of each soil from each sub-plot pool was sub-sampled,  
355 resuspended in 3.0 mL phosphate buffered saline (PBS) (1% weight/vol slurry) and  
356 either treated with 40 µM propidium monoazide (PMA) in the dark, or left untreated as a  
357 control. Both treated and untreated samples were vortexed in the dark for 4 minutes and  
358 exposed to a 650-watt light for 4 × 30 s light:30 s dark cycles to activate PMA in treated  
359 samples. Light-exposed samples were frozen at -20°C until DNA extraction. DNA was  
360 extracted from 800 µL of PMA treated and untreated soil slurries using a PowerSoil-htp  
361 96 well soil DNA Isolation kit (MoBio) following the manufacturer's instructions, except  
362 770 µL was used in the C2 step. All samples and 27 'no soil' negative controls were  
363 randomized into these 96 well DNA extraction plates and extracted simultaneously.

364 *Amplicon sequencing and analytical methods:* For sequence-based analyses of  
365 16S rRNA and ITS marker regions, we used the approaches described previously<sup>2</sup>.  
366 Briefly, we amplified each sample in duplicate in 25 µl PCR reactions containing: 12.5 µl  
367 of Promega GoTaq Hot Start Colorless Master Mix; 0.5 µl of each barcoded primer  
368 (bacterial 16S: 515F 5'-GTGCCAGCMGCCGCGGTAA-3' & 806R 5'-



369 GGACTACHVGGGTWTCTAAT-3'; fungal ITS: 5'-CTTGGTCATTTAGAGGAAGTAA-3' &  
370 ITS2 5'-GCTGCGTTCTTCATCGATGC-3'); 10.5 µl water; 1 µl of template DNA.  
371 Program: 94°C for 5 min, followed by 35 cycles of (94°C 45 s; 50°C 60 s; 72°C 90 s)  
372 and a final extension 72°C 10 min. Duplicate PCR reactions for each sample were  
373 pooled, cleaned and normalized using the ThermoFisher Scientific SequalPrep  
374 Normalization Plate kit. Cleaned and normalized amplicons were pooled, spiked with  
375 15% phiX and sequenced on an Illumina MiSeq using v2 500-cycle paired end kits. The  
376 samples were sequenced in four batches total – two for prokaryotes and two for fungi.  
377 The first two sequencing runs (one each for prokaryotes and fungi) contained all  
378 treatments and control samples up to and including the May 2016 samples. The last two  
379 sequencing runs (one each for prokaryotes and fungi) two contained samples collected  
380 on July 2016 and thereafter, plus control samples. We analyzed the 'no soil' controls to  
381 determine whether there were potential sequencing batch effects across the runs for  
382 prokaryotes or for fungi that could be detected in the community composition of these  
383 controls. We found no significant difference in the 'no soil' controls for prokaryotes  
384 (rarefied to 89 reads to include all controls; PERMANOVA  $R^2=0.028$ ;  $P=0.677$ ) or fungi  
385 (not rarefied to include all controls; PERMANOVA  $R^2=0.028$   $P=0.613$ ) that would be  
386 indicative of batch effects. Reads were processed as described in (ref. <sup>27</sup>). Briefly, raw  
387 amplicon sequences were demultiplexed according to the raw barcodes and processed  
388 with the UPARSE pipeline<sup>47</sup>. A database of  $\geq 97\%$  similar sequence clusters was  
389 constructed in USEARCH (Version 8)<sup>48</sup> by merging paired end reads, using a "maxee"  
390 value of 0.5 when quality filtering sequences, dereplicating identical sequences,  
391 removing singleton sequences, clustering sequences after singleton removal, and  
392 filtering out cluster representative sequences that were not  $\geq 75\%$  similar to any  
393 sequence in Greengenes (for prokaryotes; Version 13\_8)<sup>49</sup> or UNITE (for fungi)<sup>50</sup>  
394 databases. Demultiplexed sequences were mapped against the *de novo* constructed  
395 databases to generate counts of sequences matching clusters (i.e. taxa) for each  
396 sample. Taxonomy was assigned to each taxon using the RDP classifier with a  
397 threshold of 0.5<sup>51</sup> and trained on the Greengenes or UNITE databases. To normalize the  
398 sequencing depth across samples, samples were rarefied to 10,159 and 5,000  
399 sequences per sample for the 16S rRNA and ITS analyses, respectively. Functional  
400 predictions for fungal taxa were obtained using FUNGuild<sup>52</sup>.

401 *Statistical analyses:* Calculations of community dissimilarity and all other analyses  
402 were conducted on a reduced dataset because of the spatial and temporal  
403 heterogeneity. That is, we wanted to understand the temporal variation of microbes that  
404 are consistently present across the sub-plots and over time. When comparing slope  
405 differences, we included only taxa that were present on at least one slope *i*) with a  
406 mean read abundance of greater than 81 or 40 reads after rarefaction, for prokaryotes  
407 and fungi, respectively across all samples (an average of one (prokaryotes) or 0.5  
408 (fungi) reads per sub-plot, per time point); and were *ii*) present in more than 27 samples  
409 (1/3 of all samples). Second, we investigated only those taxa that were, on average,  
410  $\geq 0.1\%$  of the community across all samples. When investigating within-plot differences,  
411 we focused on only the taxa within that plot that met the above parameters. We  
412 emphasize that these filtering steps were deliberately stringent to enable robust  
413 temporal analyses of taxa that are consistently present both spatially and temporally.  
414 Bray-Curtis distances were calculated on this subset using the mctoolsR R package.

415 Bray–Curtis dissimilarities were calculated on square root transformed taxon relative  
416 abundances.

417 *Temporal analyses and network construction:* We identified significant temporal  
418 correlations in the relative abundances of individual taxa derived from soils that were  
419 treated to remove relic DNA using extended Local Similarity Analysis (eLSA)<sup>23</sup> with the  
420 following parameters: `lsa_compute -s 9 -r 9 -p perm`. We defined significant  
421 temporal associations as those with a local similarity (LS) score  $\geq 0.7$  (i.e.-strong to very  
422 strong correlations) and a  $q$  value  $\leq 0.001$ . Pairs of significantly correlated taxa were  
423 analyzed in Gephi (version 0.8.2). Network modularity was calculated by implementing  
424 the ‘modularity’ function<sup>24</sup> built in within Gephi, with a resolution setting of 1.0 for both  
425 slopes. Node IDs (individual taxa) belonging to the same module were extracted to  
426 delineate temporal patterns. Normalized relative abundances for each node ID were  
427 calculated using the tRank command in the multic R package.

428 *Random forest analysis:* For each slope, we used Random Forest<sup>53</sup> modeling to first  
429 identify those measured environmental and soil variables that were significant ( $P \leq 0.05$ )  
430 predictors of time, using time as a response variable (Supplementary Fig. 4). These  
431 significant environmental factors are expected to predict changes in module abundance  
432 over time (Supplementary Fig. 3). We then conducted a second round of Random  
433 Forests analysis with the significant environmental predictors to identify the most  
434 important environmental factors or soil characteristics that predicted the mean  
435 normalized relative abundances of each module (see ref. <sup>54</sup> for a similar approach). The  
436 importance (increase in mean square error %) and significance of each predictor was  
437 computed for each tree and averaged over the forest (9999 trees) using the rfPermute  
438 R package. Significant predictors were defined as those with a  $P$  value  $\leq 0.05$ . Samples  
439 for which environmental and soil characteristics were missing because of insufficient  
440 sample were excluded from random forest and spearman correlation analysis.

441  
442 **Data Availability:** Raw DNA sequence data, the corresponding mapfile and all soil and  
443 environmental characteristics are available on figshare.com:

444 10.6084/m9.figshare.6710087. Snow depth data are available through the Boulder  
445 Creek Critical Zone Observatory website:

446 <http://criticalzone.org/boulder/data/dataset/2423/>. Temperature data for the NFS and  
447 SFS are available through the Boulder Creek Critical Zone Observatory website  
448 <http://criticalzone.org/boulder/data/dataset/2426/>.

449  
450 **References:**

- 451  
452 1. O'Brien, S. L. *et al.* Spatial scale drives patterns in soil bacterial diversity.  
453 *Environmental Microbiology* **18**, 2039–2051 (2016).  
454 2. Carini, P. *et al.* Relic DNA is abundant in soil and obscures estimates of soil  
455 microbial diversity. *Nature Microbiology* **2**, 1–6 (2016).  
456 3. Flores, G. E. *et al.* Temporal variability is a personalized feature of the  
457 human microbiome. *Genome Biology* **15**, 531 (2014).  
458 4. Matulich, K. L. *et al.* Temporal variation overshadows the response of leaf  
459 litter microbial communities to simulated global change. *The ISME Journal* **9**,  
460 2477–2489 (2015).

- 461 5. Giovannoni, S. J. & Vergin, K. L. Seasonality in ocean microbial  
462 communities. *Science* **335**, 671–676 (2012).
- 463 6. Newton, R. J., Kent, A. D., Triplett, E. W. & McMahon, K. D. Microbial  
464 community dynamics in a humic lake: differential persistence of common  
465 freshwater phylotypes. *Environmental Microbiology* **8**, 956–970 (2006).
- 466 7. Shade, A., Caporaso, J. G., Handelsman, J., Knight, R. & Fierer, N. A meta-  
467 analysis of changes in bacterial and archaeal communities with time. **7**,  
468 1493–1506 (2013).
- 469 8. Fuhrman, J. A., Cram, J. A. & Needham, D. M. Marine microbial community  
470 dynamics and their ecological interpretation. *Nature Reviews Microbiology*  
471 **13**, 133–146 (2015).
- 472 9. Penton, C. R. *et al.* Denitrifying and diazotrophic community responses to  
473 artificial warming in permafrost and tallgrass prairie soils. *Front. Microbiol.* **6**,  
474 439–13 (2015).
- 475 10. Needham, D. M. & Fuhrman, J. A. Pronounced daily succession of  
476 phytoplankton, archaea and bacteria following a spring bloom. *Nature*  
477 *Microbiology* **1**, 1–7 (2016).
- 478 11. Li, X. *et al.* Changes in the structure and function of microbial communities in  
479 drinking water treatment bioreactors upon addition of phosphorus. *Applied*  
480 *and Environmental Microbiology* **76**, 7473–7481 (2010).
- 481 12. DeAngelis, K. M. Long-term forest soil warming alters microbial communities  
482 in temperate forest soils. **6**, 104 (2015).
- 483 13. Zhang, N., Xia, J., Yu, X., Ma, K. & Wan, S. Soil microbial community  
484 changes and their linkages with ecosystem carbon exchange under  
485 asymmetrically diurnal warming. *Soil Biology and Biochemistry* **43**, 2053–  
486 2059 (2011).
- 487 14. Schadt, C. W., Martin, A. P., Lipson, D. A. & Science, S. S. Seasonal  
488 dynamics of previously unknown fungal lineages in tundra soils. *Science*  
489 **301**, 1359–1361 (2003).
- 490 15. Kennedy, N., Brodie, E., Connolly, J. & Clipson, N. Seasonal influences on  
491 fungal community structure in unimproved and improved upland grassland  
492 soils. *Canadian Journal of Microbiology* **52**, 689–694 (2006).
- 493 16. Lipson, D. A., Schadt, C. W. & Schmidt, S. K. Changes in soil microbial  
494 community structure and function in an alpine dry meadow following spring  
495 snow melt. *Microb. Ecol.* **43**, 307–314 (2002).
- 496 17. Lipson, D. A. Relationships between temperature responses and bacterial  
497 community structure along seasonal and altitudinal gradients. *FEMS*  
498 *Microbiology Ecology* **59**, 418–427 (2006).
- 499 18. Lipson, D. A. & Schmidt, S. K. Seasonal changes in an alpine soil bacterial  
500 community in the Colorado Rocky Mountains. *Applied and Environmental*  
501 *Microbiology* **70**, 2867–2879 (2004).
- 502 19. Docherty, K. M. *et al.* Key edaphic properties largely explain temporal and  
503 geographic variation in soil microbial communities across four biomes. *PLoS*  
504 *ONE* **10**, e0135352–23 (2015).

- 505 20. Bond-Lamberty, B. *et al.* Soil respiration and bacterial structure and function  
506 after 17 years of a reciprocal soil transplant experiment. *PLoS ONE* **11**,  
507 e0150599–16 (2016).
- 508 21. Lennon, J. T., Muscarella, M. E., Placella, S. A. & Lehmkuhl, B. K. How,  
509 when, and where relic DNA affects microbial diversity. *mBio* **9**, e00637–18–  
510 14 (2018).
- 511 22. Hinckley, E.-L. S. *et al.* Aspect control of water movement on hillslopes near  
512 the rain-snow transition of the Colorado Front Range. *Hydrol. Process.* **28**,  
513 74–85 (2012).
- 514 23. Xia, L. C. *et al.* Extended local similarity analysis (eLSA) of microbial  
515 community and other time series data with replicates. *BMC Syst Biol* **5** S15–  
516 S15 (2011).
- 517 24. Blondel, V. D., Guillaume, J.-L., Lambiotte, R. & Lefebvre, E. Fast unfolding  
518 of communities in large networks. *Journal of Statistical Mechanics: Theory*  
519 *and Experiment* **10**, 10008 (2008).
- 520 25. Gabor, R. S. *et al.* Influence of leaching solution and catchment location on  
521 the fluorescence of water-soluble organic matter. *Environ. Sci. Technol.* **49**,  
522 4425–4432 (2015).
- 523 26. Brockett, B. F. T., Prescott, C. E. & Grayston, S. J. Soil moisture is the major  
524 factor influencing microbial community structure and enzyme activities  
525 across seven biogeoclimatic zones in western Canada. *Soil Biology and*  
526 *Biochemistry* **44**, 9–20 (2012).
- 527 27. Leff, J. W. *et al.* Consistent responses of soil microbial communities to  
528 elevated nutrient inputs in grasslands across the globe. *Proc. Natl. Acad.*  
529 *Sci. U.S.A.* **112**, 10967–10972 (2015).
- 530 28. Spohn, M. *et al.* Temporal variations of phosphorus uptake by soil microbial  
531 biomass and young beech trees in two forest soils with contrasting  
532 phosphorus stocks. *Soil Biology and Biochemistry* **117**, 191–202 (2018).
- 533 29. Hinckley, E.-L. S., Barnes, R. T., Anderson, S. P., Williams, M. W. &  
534 Bernasconi, S. M. Nitrogen retention and transport differ by hillslope aspect  
535 at the rain-snow transition of the Colorado Front Range. *Journal of*  
536 *Geophysical Research: Biogeosciences* **119**, 1281–1296 (2014).
- 537 30. Gabor, R. S., Eilers, K., McKnight, D. M., Fierer, N. & Anderson, S. P. From  
538 the litter layer to the saprolite: Chemical changes in water-soluble soil  
539 organic matter and their correlation to microbial community composition. *Soil*  
540 *Biology and Biochemistry* **68**, 166–176 (2014).
- 541 31. Taylor, A. E., Giguere, A. T., Zobelein, C. M., Myrold, D. D. & Bottomley, P.  
542 J. Modeling of soil nitrification responses to temperature reveals  
543 thermodynamic differences between ammonia-oxidizing activity of archaea  
544 and bacteria. *The ISME Journal* **11**, 896–908 (2016).
- 545 32. Stempfhuber, B. *et al.* pH as a Driver for ammonia-oxidizing archaea in  
546 forest soils. *Microb. Ecol.* **69**, 879–883 (2014).
- 547 33. Nicol, G. W., Leininger, S., Schleper, C. & Prosser, J. I. The influence of soil  
548 pH on the diversity, abundance and transcriptional activity of ammonia  
549 oxidizing archaea and bacteria. *Environmental Microbiology* **10**, 2966–2978  
550 (2008).

551 34. Heiss, E. M. & Fulweiler, R. W. Coastal water column ammonium and nitrite  
552 oxidation are decoupled in summer. *Estuarine, Coastal and Shelf Science*  
553 **178**, 110–119 (2016).

554 35. Schaefer, S. C. & Hollibaugh, J. T. Temperature decouples ammonium and  
555 nitrite oxidation in coastal waters. *Environ. Sci. Technol.* **51**, 3157–3164  
556 (2017).

557 36. Baran, R. *et al.* Exometabolite niche partitioning among sympatric soil  
558 bacteria. *Nature Communications* **6**, 8289 (2015).

559 37. Morris, J. J., Lenski, R. E. & Zinser, E. R. The Black Queen Hypothesis:  
560 Evolution of dependencies through adaptive gene loss. *mBio* **3**, e00036–12–  
561 e00036–12 (2012).

562 38. Bahram, M. *et al.* Structure and function of the global topsoil microbiome.  
563 *Nature* 1–24 (2018). doi:10.1038/s41586-018-0386-6

564 39. Faust, K. & Raes, J. Microbial interactions: from networks to models. *Nature*  
565 *Publishing Group* **10**, 538–550 (2012).

566 40. Zhalnina, K. *et al.* Dynamic root exudate chemistry and microbial substrate  
567 preferences drive patterns in rhizosphere microbial community assembly.  
568 *Nature Microbiology* **3**, 470–480 (2018).

569 41. Cole, J. C. & Braddock, W. A. *Geologic Map of the Estes Park 30' X 60'*  
570 *Quadrangle, North-central Colorado.* (2009).

571 42. Ohno, T. Fluorescence inner-filtering correction for determining the  
572 humification index of dissolved organic matter. *Environ. Sci. Technol.* **36**,  
573 742–746 (2002).

574 43. Weishaar, J. L. *et al.* Evaluation of specific ultraviolet absorbance as an  
575 indicator of the chemical composition and reactivity of dissolved organic  
576 carbon. *Environ. Sci. Technol.* **37**, 4702–4708 (2003).

577 44. Lawaetz, A. J. & Stedmon, C. A. Fluorescence intensity calibration using the  
578 Raman scatter peak of water. *Appl Spectrosc* **63**, 936–940 (2009).

579 45. Cory, R. M. & McKnight, D. M. Fluorescence spectroscopy reveals  
580 ubiquitous presence of oxidized and reduced quinones in dissolved organic  
581 matter. *Environ. Sci. Technol.* **39**, 8142–8149 (2005).

582 46. Zsolnay, A., Baigar, E., Jimenez, M. & Steinweg, B. Differentiating with  
583 fluorescence spectroscopy the sources of dissolved organic matter in soils  
584 subjected to drying. *Chemosphere* **38**, 45–50 (1999).

585 47. Edgar, R. C. UPARSE: highly accurate OTU sequences from microbial  
586 amplicon reads. *Nat Meth* **10**, 996–998 (2013).

587 48. Edgar, R. C. Search and clustering orders of magnitude faster than BLAST.  
588 *Bioinformatics* **26**, 2460–2461 (2010).

589 49. McDonald, D. *et al.* An improved Greengenes taxonomy with explicit ranks  
590 for ecological and evolutionary analyses of bacteria and archaea. *The ISME*  
591 *Journal* **6**, 610–618 (2011).

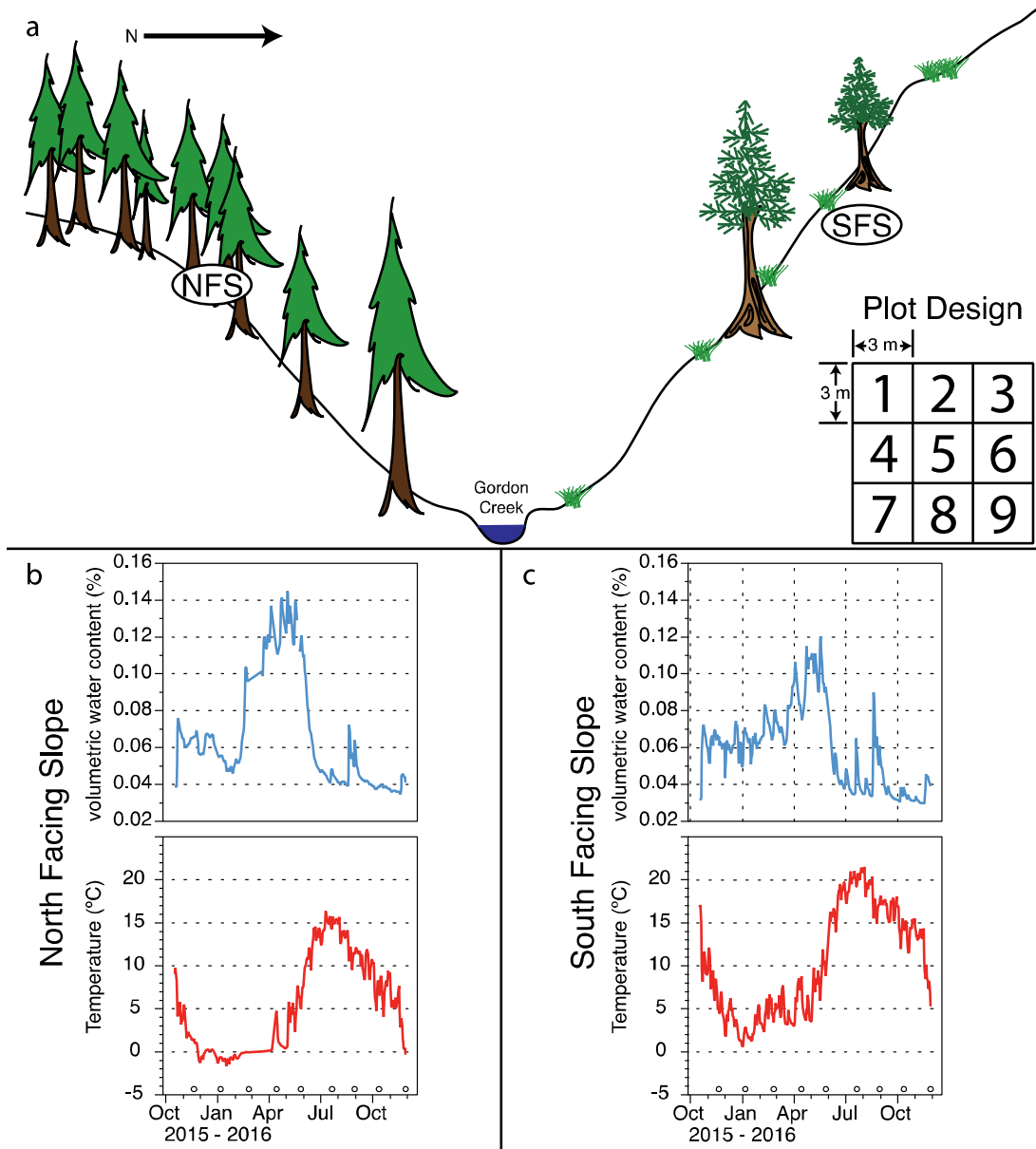
592 50. Abarenkov, K. *et al.* The UNITE database for molecular identification of  
593 fungi--recent updates and future perspectives. *New Phytol.* **186**, 281–285  
594 (2010).

- 595 51. Wang, Q., Garrity, G. M., Tiedje, J. M. & Cole, J. R. Naive Bayesian  
596 classifier for rapid assignment of rRNA sequences into the new bacterial  
597 taxonomy. *Applied and Environmental Microbiology* **73**, 5261–5267 (2007).
- 598 52. Nguyen, N. H. *et al.* FUNGuild: An open annotation tool for parsing fungal  
599 community datasets by ecological guild. *Fungal Ecology* **20**, 241–248  
600 (2016).
- 601 53. Breiman, L. Random Forests. *Machine Learning* **45**, 5–32 (2001).
- 602 54. Delgado-Baquerizo, M. *et al.* Differences in thallus chemistry are related to  
603 species-specific effects of biocrust-forming lichens on soil nutrients and  
604 microbial communities. *Funct Ecol* **29**, 1087–1098 (2015).
- 605  
606

607 **Acknowledgements:** We thank Gordon Bowman, Youchao Chen, Matt Gebert,  
608 Rebecca Gross, Evan Lih, Emily Morgan, Dillon Ragar, Nathan Rock and Joel Singley  
609 for assistance setting up plots, sampling and nutrient analyses. We also thank David  
610 Needham for assistance with LSA and Albert Barberán for critical feedback on the  
611 manuscript. Funding to support this work was provided by grants from the National  
612 Science Foundation EAR 1331828, EAR 1461281, and DEB 1556753 to N.F., and a  
613 Visiting Postdoctoral Fellowship award to P.C. from the Cooperative Institute for  
614 Research in Environmental Sciences at the University of Colorado.

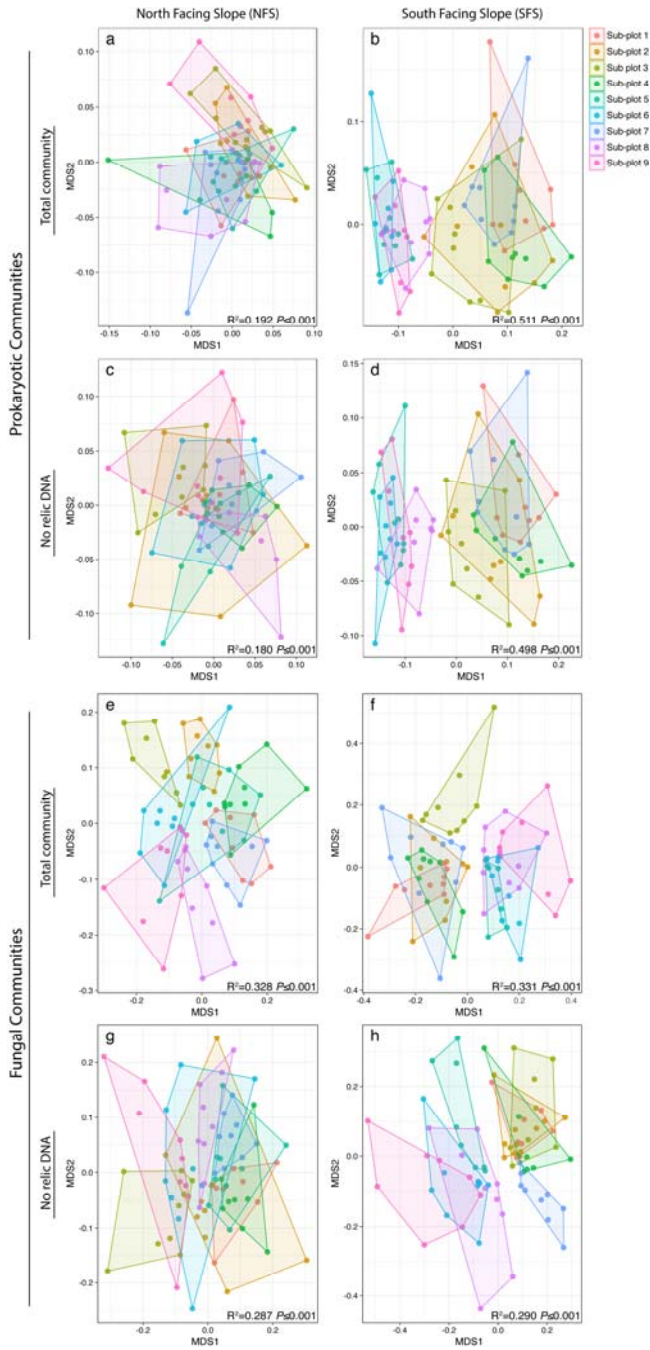
615

Figures:



617  
 618  
 619  
 620  
 621  
 622  
 623  
 624  
 625  
 626  
 627  
 628  
 629  
 630

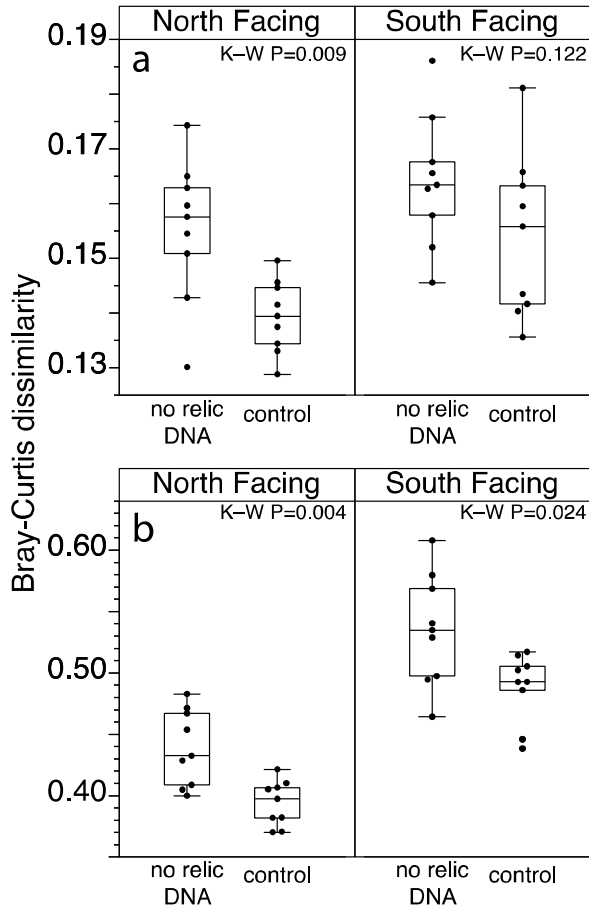
**Figure 1:** Overview of the Gordon Gulch sampling sites and environmental conditions across the sampling sites. (a) Conceptual diagram of sampling site location and plot design, reproduced with modification from<sup>29</sup>. The North facing slope (NFS) plot was centered at 40°0'44.759"N 105°28'9.123"W. The South facing slope (SFS) plot was centered at 40°0'48.551"N 105°28'8.355"W. Inset in (a) is an illustration of plot design. A single plot is comprised of nine 3 m x 3 m sub-plots. Numbers represent replicate sub-plots as described in the main text. Daily mean soil volumetric water content and soil temperature from *in situ* sensors at 5 cm depth for the NFS (b) and SFS (c) during the course of the experiment. Small circles on the temperature plots in (b) and (c) indicate sampling dates.



631  
632  
633  
634  
635  
636  
637  
638

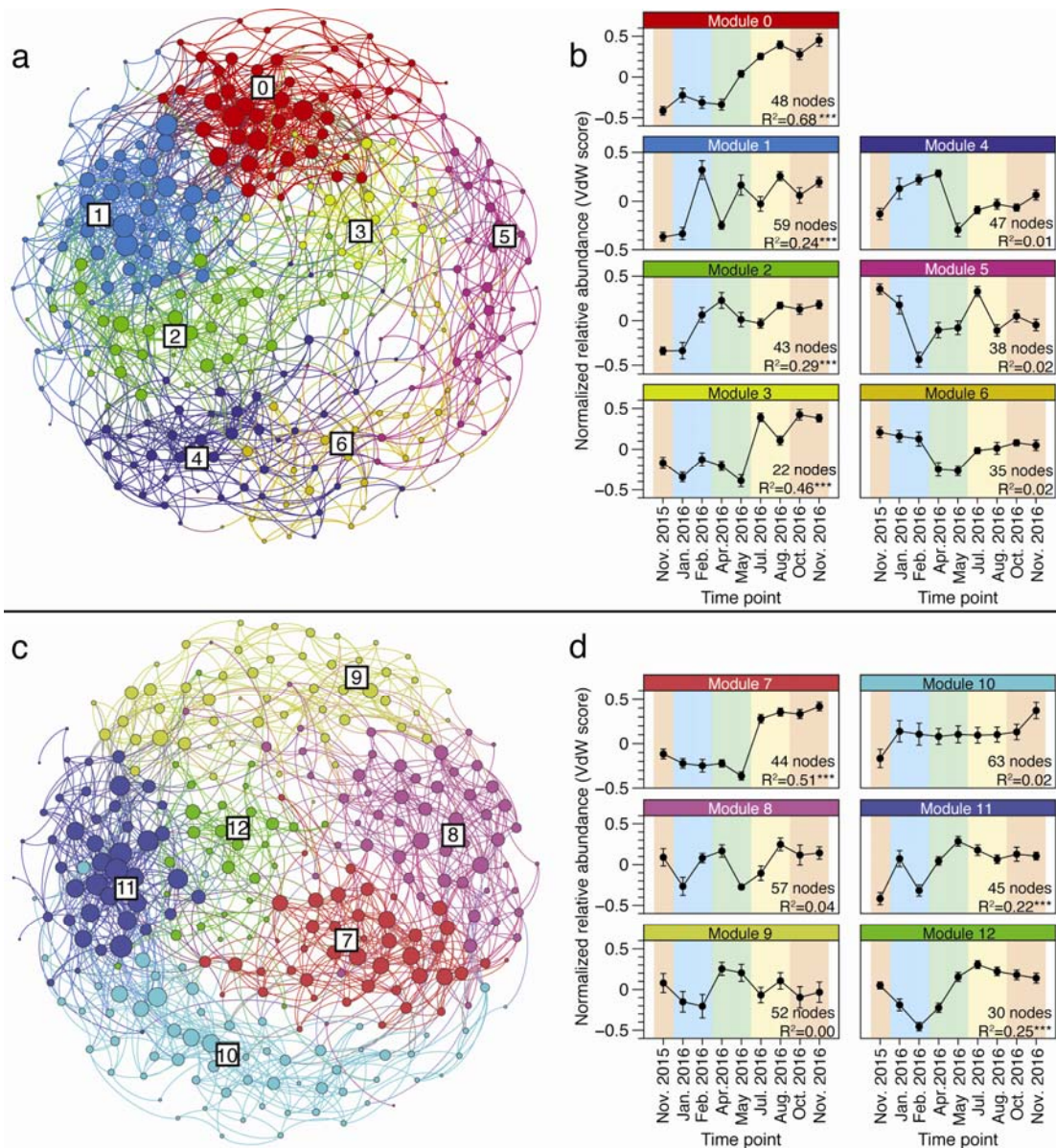
**Figure 2:** Intra-plot spatial variability in soil microbial communities persists over time on both slopes regardless of whether relic DNA is removed. NMDS plots showing the prokaryotic (a-d) or fungal (e-h) communities on the north facing slope (a,c,e,g) and south facing slope (b,d,f,h). Points are colored by sub-plot number (plot layout is illustrated in Figure 1 in the main text). Hulls connect the outermost points on each slope. PERMANOVA statistics are listed on each panel.





639  
 640  
 641  
 642  
 643  
 644  
 645  
 646  
 647

**Figure 3:** Soils without relic DNA were found to harbor microbial communities that are more dissimilar over time than in control soils containing relic DNA. (a) Prokaryotes (b) Fungi. Points are the mean community dissimilarity for a given sub-plot across all time points (n=9) for samples after relic DNA removal (no relic DNA) or untreated samples (control). Box plots illustrate interquartile range  $\pm$  1.5  $\times$  interquartile range. The horizontal line in each box plot is the median. Outliers ( $>1.5 \times$  interquartile range) are shown as points outside of whiskers. Kruskal-Wallis test (K-W) P values are shown.



648

649

650

651

652

653

654

655

656

657

658

659

660

661

662

**Figure 4:** Cross-domain temporal dynamics in belowground microbial communities reveals temporal niche structure. Correlation networks based on significant microbe-microbe temporal correlations for the NFS (a) and SFS (c). Nodes in (a) & (c) are individual prokaryotic or fungal taxa. Lines between nodes represent significant ( $q$  value  $\leq 0.001$ ) and strong (local similarity score  $\geq 0.7$ ) positive temporal correlations. The sizes of nodes are proportional to the number of correlations to other nodes (the degree), whereby larger nodes have more connections. Colors represent distinct modules, as determined using the modularity algorithm described in ref. <sup>24</sup>. Boxed numbers in networks are arbitrary module numbers and match those in panels (b) and (d). Modularity analysis of each network revealed clusters of microbes that have similar temporal patterns. These temporal patterns were plotted for the NFS (b) and SFS (d). Points in (b) and (c) are the mean Van der Waerden (VdW) normalized relative abundance of all taxa in a given module. Error bars show  $\pm$  SEM. The number of nodes included in each module and the PERMANOVA P value describing the relationship of

663 the normalized relative abundances in relation to time are shown. P values marked with  
664 asterisks are significant at  $P \leq 0.001$ . Background is shaded by season: orange=autumn;  
665 blue=winter; green=spring; yellow=summer. See Supplementary Table 1 for taxonomic  
666 module membership.